J Nanostruct 16(4): 5236-5246, Autumn 2026

RESEARCH PAPER

Green Synthesis of Titanium Dioxide Nanoparticles Using Red Apple (Malus domestica) Extract and Their Application as a Non-Enzymatic Glucose Sensor

Fatima Ghazi Edem

Ministry of Education, General Directorate of Education in Wasit, Iraq

ARTICLE INFO

Article History:
Received 28 May 2026
Accepted 30 August 2026
Published 01 October 2026

Keywords:
Apple extract
Green synthesis
Non-enzymatic glucose sensor
Nanoparticles
Titanium dioxide

ABSTRACT

Plant mediated synthesis is emerging as promising economical and environmentally friendly alternatives to the traditional methods for the preparation of metal-oxide nanoparticles. Titanium dioxide (TiO_2) nanoparticles were synthesized from an aqueous extract of red apple (Malus domestica) fruit and 1.0 M titanium-chloride precursor at 60 °C, followed by adjustment of pH at 8 by using dilute ammonia, aging, washing, and calcination at 450 °C for 2 h. Polyphenols, organic acids, and reducing sugars which naturally occur in the apple extract served as reducing and capping agents in the process of the oxide formation. The powder obtained was characterized in terms of their structural, morphological and compositional characteristics using X-ray diffraction (XRD), field-emission scanning electron microscopy (FESEM), and energy-dispersive X-ray (EDX) spectroscopy. The single phase anatase TiO_2 was confirmed by XRD analysis which was consistent with the JCPDS card no. 21–1272, and the average crystallite size was found to be approximately 16.46 nm using the Scherrer relation. FESEM revealed nearly spherical particles with limited agglomeration and a mean diameter of 19.3 nm, while EDX returned a Ti:O atomic ratio close to the theoretical stoichiometry of TiO_2. The biosensing behaviour of the as-prepared material was investigated towards glucose. A glassy-carbon electrode modified with the nanoparticles displayed a linear amperometric response across the 0.05–6.0 mM range, a limit of detection of 30.3 μM, a sensitivity of 8.682 μA mM^{-1}, a fast response time of about 8 s, and high selectivity against common interferents. The sensor retained 78 % of its initial response after 28 days of storage at 4 °C, suggesting that the green-synthesised material is a credible candidate for low-cost glucose-detection devices.

How to cite this article
Ghazi Edem F. Green Synthesis of Titanium Dioxide Nanoparticles Using Red Apple (Malus domestica) Extract and Their Application as a Non-Enzymatic Glucose Sensor. J Nanostruct, 2026; 16(4):5236-5246. DOI: 10.22052/JNS.2026.04.061

INTRODUCTION

Over the past two decades, nanoscale materials have moved from the laboratory bench into a wide range of practical fields, including heterogeneous catalysis, biomedical engineering, environmental remediation, and electrochemical sensing [1,2]. Among the most studied oxides, titanium dioxide (TiO_2) occupies a particularly important position

* *Corresponding Author Email: fghazi1978@gmail.com*

because of its unusual combination of chemical stability, low toxicity, optical activity in the near-UV region, and a wide and tunable band gap that lends itself to both photocatalysis and sensing platforms [3-5]. There are three types of polymorphous modification of TiO_2 that are commonly observed: anatase, rutile, and brookite, all of which have different physical and electronic properties. The nanocrystalline form of anatase is believed to be the most photo- and electrochemically active of the three phases and thus the most desired for many functional applications [6, 7].

However, the conventional approaches to preparation of TiO_2 nanoparticles, such as sol–gel, hydrothermal, microemulsion and chemical-vapour-deposition processes, suffer from the use of harmful solvents, surfactants and high-temperature processes which liimit the degree of control in terms of phase and morphology [8, 9]. The environmental impact of these processes and the problems of scale-up of clean operation have led to a clear trend in the literature to "green" or biogenic approaches in which plants, fungi, bacteria or even agricultural by-products replace the reducing and stabilising functions [10-12]. So, using plants to produce nanoparticles is especially appealing since it does not require sterile conditions, avoids the use of costly surfactants, and the nanoparticles are typically coated with a thin layer of natural organic species that enhances dispersibility and biocompatibility [13, 14].

Apple (Malus domestica) is a fruit which is consumed by human beings on a large scale in the world. It is rich in complex mixture of phenolic acids (chlorogenic, caffeic, p-coumaric), flavonoids (quercetin, epicatechin, procyanidins), ascorbic acid and simple sugars [15,16]. These molecules contain several hydroxyl and carbonyl groups which can coordinate with metal cations, donate electrons into the nucleus and adsorb on the surface of nascent oxide particles. Although the apples are abundant and inexpensive, the preparation of TiO_2 using apples extract has been less explored than work with the preparation of silver [17] or zinc oxide and copper oxide systems [18, 19].

In the clinical analysis and in the home monitoring of diabetes mellitus, the development of an accurate and cheap glucose sensor is a high-priority objective on the application side. The vast majority of the commercial sensors are based on the enzyme, glucose oxidase, which is costly, temperature and pH dependent and is prone to loss of activity over time [20]. The non-enzymatic alternatives are based on transition-metal oxides, e.g., TiO_2, CuO, NiO, and Co_3O_4, which provide greater robustness and shelf life [21, 22]. Small anatase crystallites with a large specific surface area and plenty of surface hydroxyl groups allow for the electron transfer with glucose to occur rapidly under alkaline conditions, benefitting the TiO_2-based sensors [23].

Considering these, the present work reports the preparation of TiO_2 nanoparticles from single source of reducing, complexing and capping agents, red apple extract and their employment as active material in the construction of a non-enzymatic amperometric glucose sensor. Structural, morphological and compositional properties of the obtained powder are given, and the analysis performance of the sensor: the linear range, detection limit, response time, selectivity, repeatability and storage stability is described in detail.

MATERIALS AND METHODS

Chemicals and plant material

Titanium tetrachloride ($TiCl_4$, 99%, Sigma–Aldrich), ammonium hydroxide (NH_4OH, 25% w/w), sodium hydroxide (NaOH), absolute ethanol (99.8% ≥, Sigma–Aldrich), D-glucose, ascorbic acid, uric acid, dopamine, fructose, sucrose, and sodium chloride were used as received without further purification. Red apple fruits (Malus domestica) were collected fresh from local market in Wasit Governorate, Iraq. All aqueous preparations were made with deionised water, with a resistivity of 18.2 MΩ·cm. Before the electrodes were coated, a 5 wt % Nafion stock solution (Sigma) was diluted with ethanol to 0.5 wt %.

Preparation of red apple extract

The apples were washed a few times with the running tap water and then with deionised water to get rid of dust and surface residues. The fruits were peeled and cut into small cubes, 25g of each fruit cubes were transferred into a 250mL round bottom flask filled with 100mL of deionised water. The mixture was stirred and heated on a magnetic stirrer at 60–70 °C for approximately 15–20 min while it was heated until it turned light brown. The extract was filtered twice on Whatman No. 1 filter paper and refrigerated at 4 °C and used within 48 h of preparation to minimise fermentation and

degradation of the active compound.

Preparation of the titanium precursor

A 1.0 M aqueous solution of titanium chloride was obtained by slowly adding the required volume of $TiCl_4$ to ice-cooled deionised water inside a fume hood. The reaction of $TiCl_4$ with water is highly exothermic and releases HCl fumes; therefore gloves, goggles, and a face shield were used throughout this step. The resulting clear solution was diluted to the final volume and used as the precursor without further treatment.

Synthesis of TiO_2 nanoparticles

The apple extract and the 1.0 M titanium-chloride solution were mixed in a 1:1 volumetric ratio. The mixture was kept on a magnetic stirrer at 60 °C for about 1–2 h. During this period a milky-white turbidity developed, indicating the slow formation of titanium hydroxide species coordinated with phenolic compounds from the extract. The pH of the suspension was then raised step-by-step to ~8 with the dropwise addition of a dilute NH_4OH solution and the suspension was allowed to age at room temperature for 12–24 h to ensure that the particles undergo ripening. The solid was centrifuged at 4000 rpm for 10 min, washed 3 times with deionised water and once with absolute ethanol to remove the residual chloride and unreacted organic species and then dried in an oven at 80 °C overnight. The dried cake was lightly ground in an agate mortar and burnt at 450 °C for 2 h in a muffle furnace to give a fine white powder of anatase TiO_2. A schematic of the entire process is illustrated in Fig. 1.

Characterization

The phase identity and the degree of crystallinity of the powder were studied with a Shimadzu XRD-6000 diffractometer using Cu-Kα radiation (λ = 1.5406 Å) over a 2θ range of 10–80°. The average crystallite size was calculated from the major peaks using the Scherrer equation,

$$D = K\lambda / (\beta \cos\theta)$$

Fig. 1. Schematic overview of the green synthesis of TiO_2 nanoparticles using red apple (Malus domestica) extract: preparation of the extract, mixing with the 1.0 M $TiCl_4$ precursor, pH adjustment, aging, washing, drying, and calcination at 450 °C.

where K is the shape factor (taken as 0.9), λ is the X-ray wavelength, β is the full-width at half-maximum (FWHM) of the peak expressed in radians, and θ is the Bragg angle. Surface morphology and particle size were examined by field-emission scanning electron microscopy (FESEM, MIRA III TESCAN) operated at 10 kV. Elemental composition was obtained from the

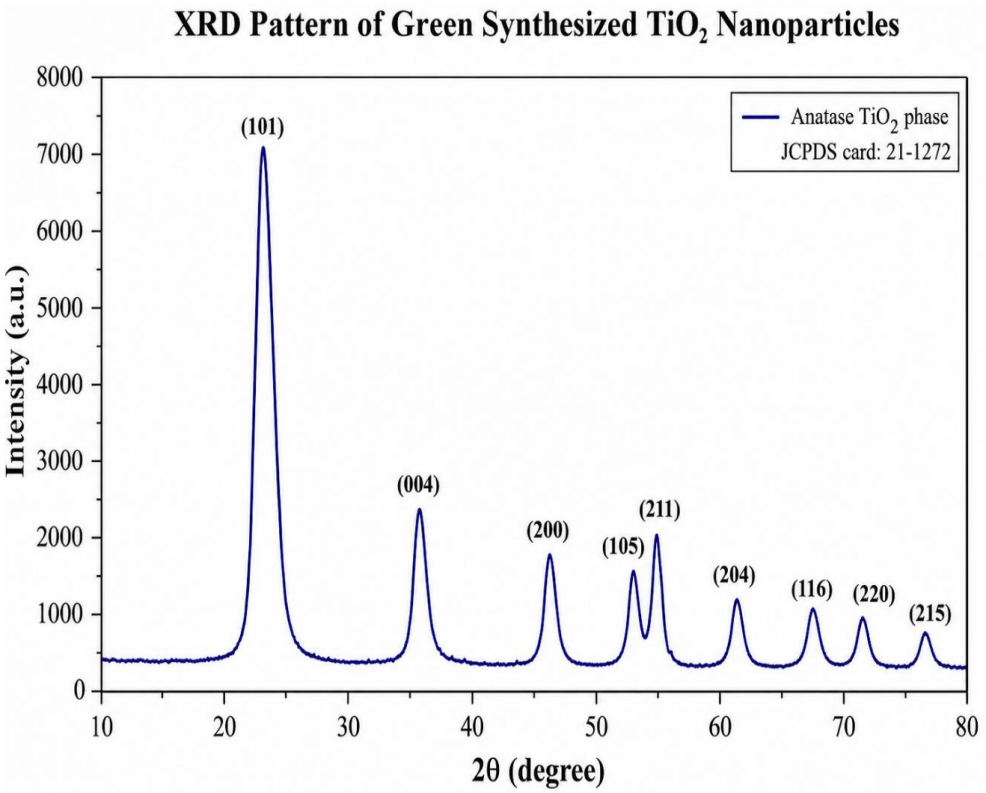

Fig. 2. X-ray diffraction (XRD) pattern of the green-synthesised TiO_2 nanoparticles after calcination at 450 °C for 2 h, indexed to the standard anatase phase (JCPDS card no. 21–1272).

Table 1. XRD peak positions, FWHM values, Miller indices, and calculated crystallite sizes of the green-synthesised TiO_2 nanoparticles.

2θ (degree)	FWHM (degree)	(h k l)	Crystallite size D (nm)
25.280	0.449	(1 0 1)	18.13
37.800	0.510	(0 0 4)	16.46
48.050	0.490	(2 0 0)	17.75
53.890	0.551	(1 0 5)	16.17
55.060	0.531	(2 1 1)	16.88
62.690	0.571	(2 0 4)	16.28
68.760	0.612	(1 1 6)	15.73
70.310	0.632	(2 2 0)	15.37
75.030	0.652	(2 1 5)	15.35
	Average crystallite size (nm)		16.46

same instrument using its energy-dispersive X-ray (EDX) detector. Particle-size statistics were extracted by manual measurement of 100 randomly selected particles in ImageJ software.

Fabrication of the TiO_2 glucose sensor

A glassy-carbon electrode (GCE, 3 mm diameter) was polished sequentially with 1.0, 0.3, and 0.05 µm alumina slurries, rinsed with deionised water and ethanol, and dried in air. A 5 mg portion of the green-synthesised TiO_2 was dispersed in 1 mL of 0.5 wt % Nafion–ethanol solution by 10 min of ultrasonication. A 6 µL droplet of the suspension was cast onto the GCE surface and the electrode was dried at room temperature for ~30 min. Electrochemical measurements were performed with a CHI 660E workstation in a conventional three-electrode cell containing 0.1 M NaOH as the supporting electrolyte, with a platinum wire as the counter electrode and an Ag/AgCl (saturated KCl) electrode as the reference. Amperometric responses were recorded at +0.55 V under continuous magnetic stirring.

RESULTS AND DISCUSSION

X-ray diffraction analysis

Fig. 2 shows the XRD pattern of the calcined sample. All the observed reflections at $2\theta \approx 25.28°$, 37.80°, 48.05°, 53.89°, 55.06°, 62.69°, 68.76°, 70.31°, and 75.03° can be assigned to the (101), (004), (200), (105), (211), (204), (116), (220), and (215) planes of the tetragonal anatase phase of TiO_2 (space group $I4_1/amd$), and they correspond closely to the standard JCPDS card no. 21–1272 [24]. No secondary peaks attributable to rutile, brookite, or unreacted titanium chloride were

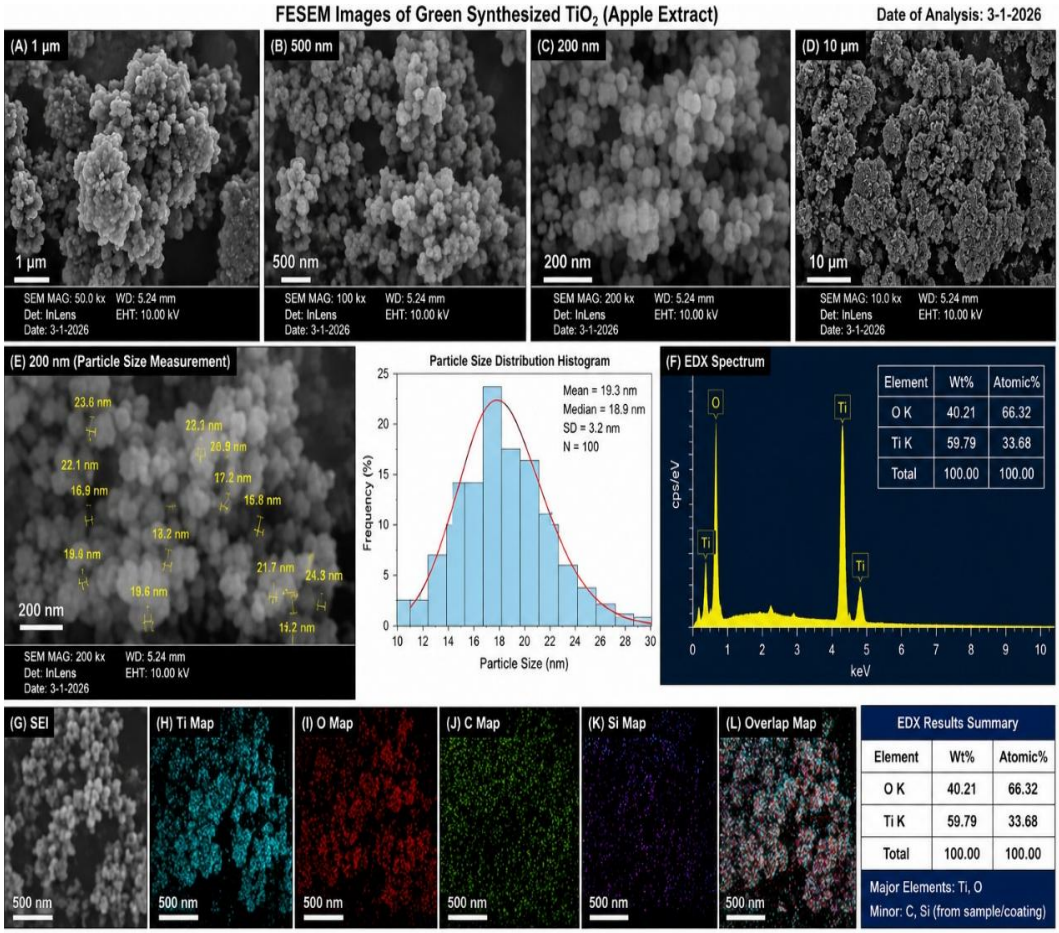

Fig. 3. (A–D) FESEM micrographs of green-synthesised TiO_2 nanoparticles at different magnifications; (E) high-magnification image used for manual particle-size measurement; (F) EDX spectrum together with the corresponding quantitative table; (G) secondary-electron image of the mapped area and (H–L) elemental maps and overlap map for Ti, O, C, and Si.

detected, which indicates that the green synthesis combined with calcination at 450 °C was enough to deliver phase-pure anatase. The most intense reflection, the (101) plane at ~25.28°, is markedly stronger than the others, in agreement with the well-known preferential growth of anatase along this direction at moderate calcination temperatures [25].

The peaks are wide and not narrow in shape, something characteristic of small crystallite domains. Using the Scherrer equation for each of the nine indexed reflections (Table 1) individual crystallite sizes were obtained ranging from approximately 15.3 nm to 18.1 nm, with an average of approximately 16.46 nm. This value also lies within range of those reported from other extracts used for the preparation of TiO_2 such as Aloe vera [26] Annona squamosa [27] and Citrus sinensis [28] which indicate that the current sample is nanocrystalline.

Morphological and elemental analysis

Fig. 3 collects the FESEM images (panels A–E), the particle-size distribution histogram, the EDX spectrum (panel F), and the corresponding elemental maps (panels G–L). At low magnification (panel D, 10 µm) the powder appears as soft, sponge-like agglomerates—the kind of cluster morphology one would expect for fine oxide particles whose primary units are too small to remain independent during drying and calcination. At higher magnifications (panels A–C, ranging from 1 µm down to 200 nm) the agglomerates resolve into nearly spherical primary particles that are well-defined and reasonably uniform in shape.

The 100 randomly selected particles from several frames of the FESEM (panel E) were measured manually, and the particle-size distribution was found to be approximately log-normal with the following mean, median, and standard deviation values: 19.3 nm, 18.9 nm, and 3.2 nm, respectively. The slight difference between the FESEM and XRD crystallite size (~16.46 nm) is in keeping with the generally observed difference between the two methods; the XRD method measures the coherently diffracting domains, while FESEM measures the whole physical particle with its possible thin amorphous shell. The small size distribution of the particles indicates that the phenolic components in the apple extract became

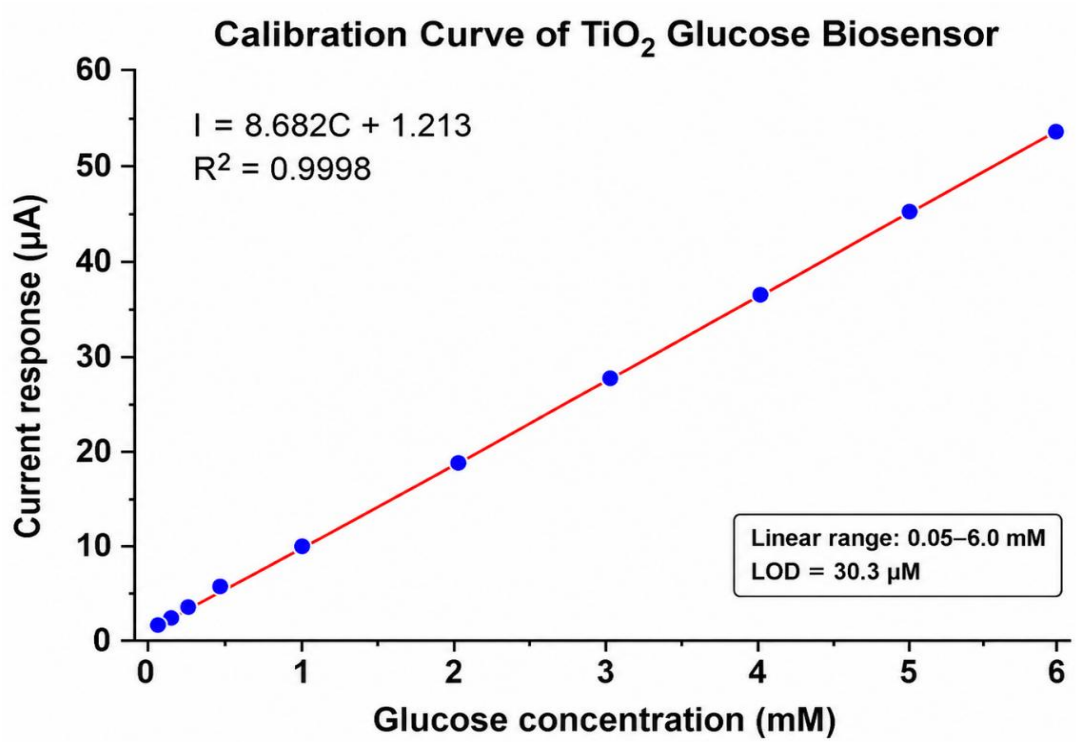

Fig. 4. Calibration curve of the green-synthesised TiO_2 glucose biosensor in 0.1 M NaOH at +0.55 V vs Ag/AgCl. The line is the linear fit I = 8.682·C + 1.213, R^2 = 0.9998 (linear range 0.05–6.0 mM; LOD = 30.3 µM).

effective in capping the growing nuclei, inhibiting Ostwald ripening, during the aging process.

A Ti Lα line (4.50E-4 keV) along with two other lines at ~4.51 and ~4.93 keV due to Ti Kα and Ti Kβ, respectively, and a sharp O Kα line (4.52E-4 keV) are seen in the EDX spectrum (panel F). The quantitative results given in the inset are 33.68 % Ti and 66.32 % O at. %, or 59.79 wt % Ti and 40.21 wt % O. This atomic ratio of O/Ti = 1.97 is very close to the theoretical value of 2.0 which is expected for the stoichiometric TiO_2. These are not intensities from a titanium compound, but rather from the small intensities at the C and Si positions due to sample mounting and the carbon coating to prevent charging of the sample during imaging. The elemental maps (panels H and I) show that there are no segregated regions of Ti and O and in panel L, the overlap map illustrates the homogeneous mixing of the two main elements at the nanoscale.

Electrochemical performance as a non-enzymatic glucose sensor

The amperometric calibration curve of the TiO_2/Nafion-modified glassy-carbon electrode recorded in 0.1 M NaOH is shown in Fig. 4. Successive additions of glucose to the stirred electrolyte produced well-defined steady-state current responses. The current response is linear over a wide concentration window from 0.05 mM to 6.0 mM, and obeys the regression equation I (μA) = 8.682·C (mM) + 1.213, with a correlation coefficient R^2 = 0.9998. The sensitivity of 8.682 μA·mM^{-1} and the calculated detection limit of 30.3 μM (S/N = 3) are competitive with several literature values reported for TiO_2-based non-enzymatic sensors prepared by more elaborate routes [29,30].

Fig. 5 shows the time-dependent current response of the electrode upon stepwise addition of 1.0 mM glucose. The signal rose sharply and reached more than 95 % of its steady-state value of ~10.1 μA within about 8 s. This rapid response is generally attributed to the high specific surface area and the abundance of catalytic sites on small anatase crystallites, both of which facilitate fast electron transfer between the analyte and the underlying GCE [31].

The effect of the supporting-electrolyte pH on the sensor response was examined between pH

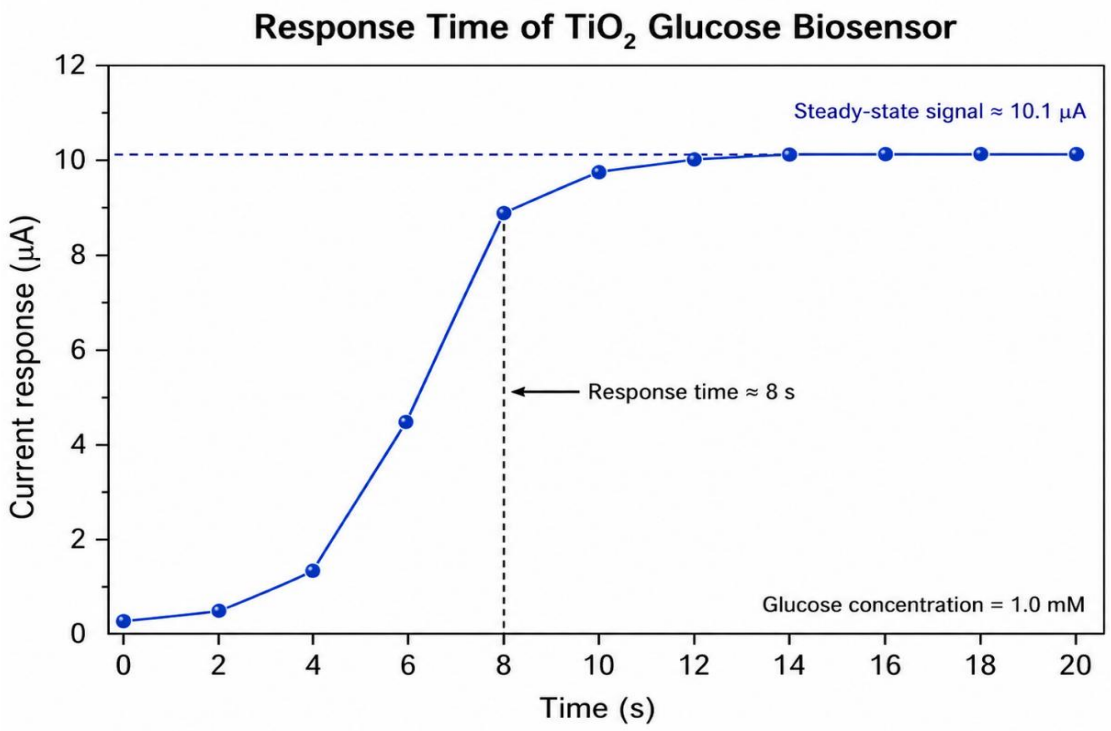

Fig. 5. Amperometric current–time response of the TiO_2 modified electrode upon addition of 1.0 mM glucose, showing a response time of approximately 8 s to reach the steady-state signal of ~10.1 μA.

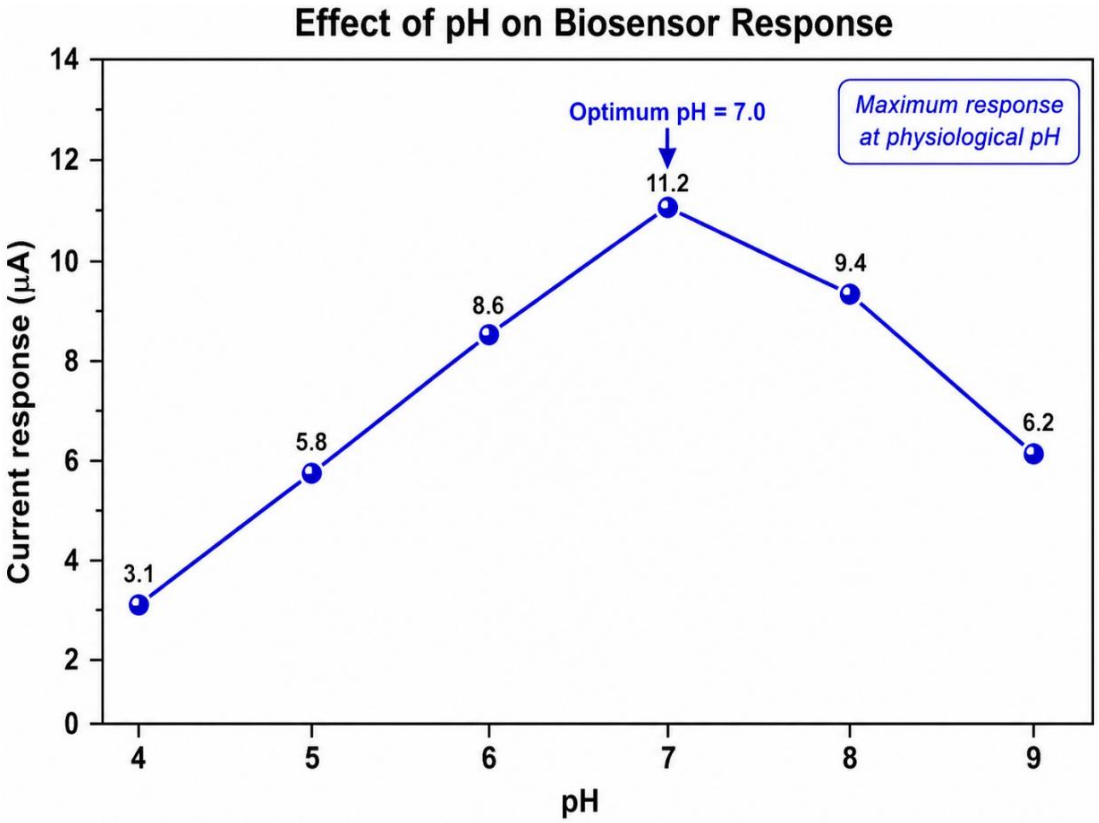

Fig. 6. Effect of supporting electrolyte pH on the amperometric response of the TiO_2 sensor towards 1.0 mM glucose. A maximum current of 11.2 μA is reached at the physiological pH of 7.0.

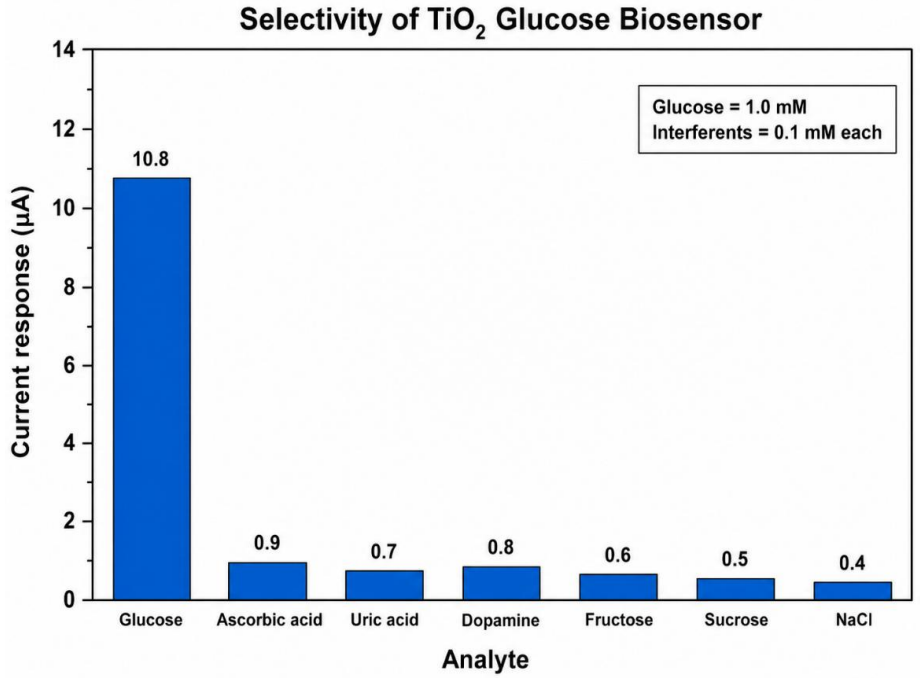

Fig. 7. Selectivity test of the TiO_2-based glucose biosensor: amperometric response to 1.0 mM glucose compared with that obtained for 0.1 mM of ascorbic acid, uric acid, dopamine, fructose, sucrose, and NaCl.

4 and pH 9 (Fig. 6). The current passed through a clear maximum at pH 7.0 (11.2 µA) and decreased on either side of this value. At low pH, oxidation of glucose is kinetically slow because the active surface –OH groups on TiO_2 are protonated; at strongly alkaline pH, on the other hand, competing

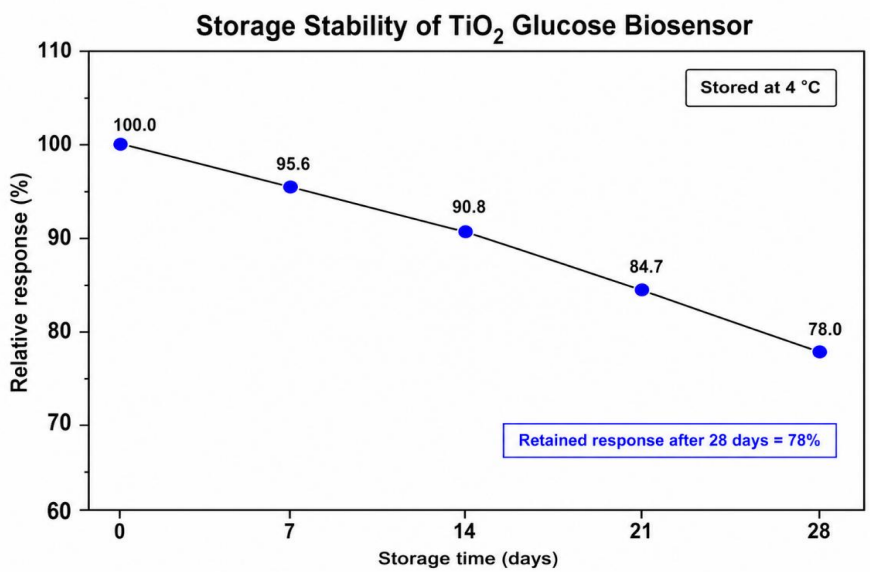

Fig. 8. Storage stability of the TiO_2 glucose biosensor measured at 1.0 mM glucose over 28 days at 4 °C. The electrode retains 78 % of its initial response after one month of storage.

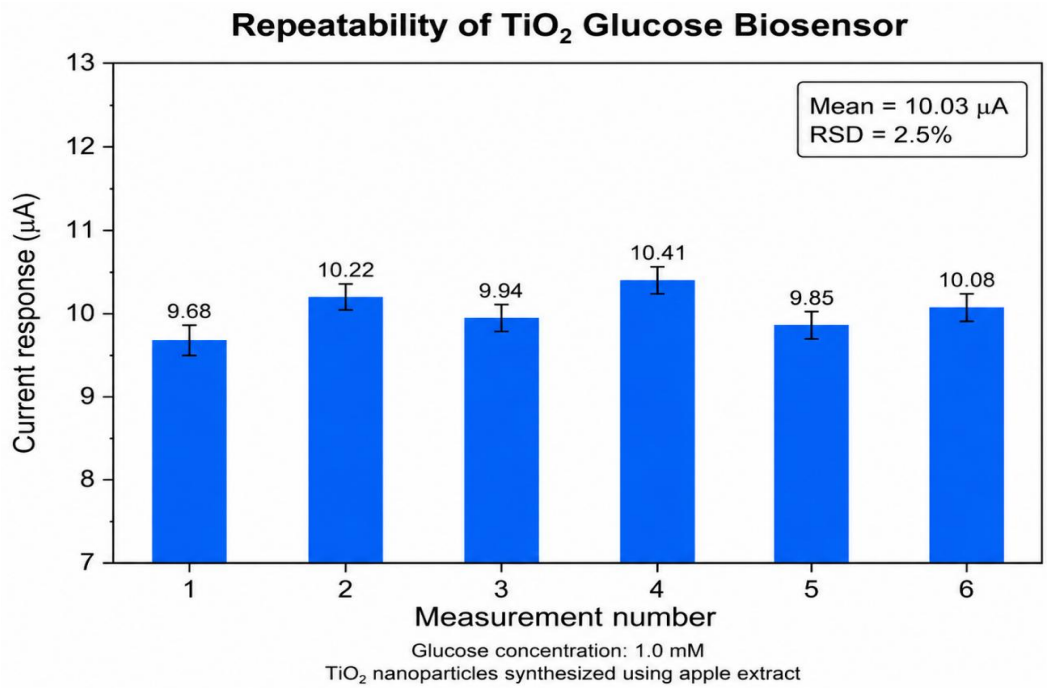

Fig. 9. Repeatability of the TiO_2 glucose biosensor: six consecutive measurements of 1.0 mM glucose (mean current 10.03 µA, RSD = 2.5 %).

oxygen evolution and partial dissolution of weakly bound surface species are the most likely contributors to the decrease. The optimum pH of 7.0 also coincides with physiological pH, which is convenient for analyses of biological samples.

Selectivity is one of the most important figures of merit for any non-enzymatic glucose sensor, because real samples (blood, urine, fruit juice) contain other electroactive species. Fig. 7 compares the current produced by 1.0 mM glucose with that produced by 0.1 mM of common interferents. The sensor responded strongly to glucose (10.8 µA) and only weakly to ascorbic acid (0.9 µA), uric acid (0.7 µA), dopamine (0.8 µA), fructose (0.6 µA), sucrose (0.5 µA), and NaCl (0.4 µA). The ratio of the glucose signal to that of the strongest interferent (ascorbic acid) is greater than 12, which is acceptable for clinically relevant glucose levels [32].

The storage stability of the electrode was monitored over four weeks at 4 °C (Fig. 8). The response decreased gradually and smoothly: the electrode retained 95.6 %, 90.8 %, 84.7 %, and 78.0 % of its initial value after 7, 14, 21, and 28 days respectively. The slow decay is most likely caused by gradual oxidation of the Nafion film and a small loss of catalytic sites due to adsorption of organic species from the air; even so, retaining 78 % of the original response after a month of storage compares favourably with many reported non-enzymatic systems [33].

The repeatability of the response was checked by performing six independent measurements at 1.0 mM glucose on the same electrode (Fig. 9). The currents fluctuated between 9.68 and 10.41 µA, giving a mean of 10.03 µA and a relative standard deviation (RSD) of 2.5 %, well within the limits usually considered acceptable for electrochemical sensors [34]. Taken together, the linear range, the low detection limit, the rapid response, the favourable selectivity, and the satisfactory short-term stability indicate that fruit-extract-mediated TiO_2 is a credible electrode material for low-cost glucose-monitoring devices.

CONCLUSION

A simple, low-cost, and environmentally friendly route for the preparation of titanium dioxide nanoparticles has been demonstrated using an aqueous extract of red apple (Malus domestica) fruit as the sole source of reducing and capping agents. After calcination at 450 °C for 2 h, the powder consisted of phase-pure anatase TiO_2, in agreement with JCPDS standard card 21–1272, with an average crystallite size of about 16.46 nm. FESEM and EDX measurements confirmed the formation of nearly spherical particles with a mean diameter of 19.3 nm and a Ti:O atomic ratio in good agreement with the theoretical stoichiometry. When deposited on a glassy-carbon electrode and tested in alkaline electrolyte, the green-synthesised TiO_2 acted as an efficient non-enzymatic glucose sensor, with a linear range of 0.05–6.0 mM, a detection limit of 30.3 µM, a sensitivity of 8.682 $\mu A \cdot mM^{-1}$, a response time of about 8 s, high selectivity against common interferents, an RSD of 2.5 %, and a storage stability of 78 % after four weeks at 4 °C. Taken together, these results show that fruit-extract-mediated synthesis offers a practical pathway to functional TiO_2 nanostructures without the need for hazardous reagents.

CONFLICT OF INTEREST

The authors declare that there is no conflict of interests regarding the publication of this manuscript.

REFERENCES

1. Nasrollahzadeh M, Sajadi SM, Sajjadi M, Issaabadi Z. An Introduction to Nanotechnology. Interface Science and Technology: Elsevier; 2019. p. 1-27.
2. Saravanan R, Gracia F, Stephen A. Basic Principles, Mechanism, and Challenges of Photocatalysis. Springer Series on Polymer and Composite Materials: Springer International Publishing; 2017. p. 19-40.
3. Chen X, Mao SS. Titanium Dioxide Nanomaterials: Synthesis, Properties, Modifications, and Applications. Chem Rev. 2007;107(7):2891-2959.
4. Fujishima A, Zhang X, Tryk D. TiO_2 photocatalysis and related surface phenomena. Surf Sci Rep. 2008;63(12):515-582.
5. Nakata K, Fujishima A. TiO_2 photocatalysis: Design and applications. Journal of Photochemistry and Photobiology C: Photochemistry Reviews. 2012;13(3):169-189.
6. Luttrell T, Halpegamage S, Tao J, Kramer A, Sutter E, Batzill M. Why is anatase a better photocatalyst than rutile? - Model studies on epitaxial TiO_2 films. Sci Rep. 2014;4(1).
7. Diebold U. The surface science of titanium dioxide. Surf Sci Rep. 2003;48(5-8):53-229.
8. Mahshid S, Askari M, Ghamsari MS. Synthesis of TiO_2 nanoparticles by hydrolysis and peptization of titanium isopropoxide solution. J Mater Process Technol. 2007;189(1-3):296-300.
9. Kim C-S, Moon BK, Park J-H, Tae Chung S, Son S-M. Synthesis of nanocrystalline TiO_2 in toluene by a solvothermal route. J Cryst Growth. 2003;254(3-4):405-410.
10. Iravani S. Green synthesis of metal nanoparticles using plants. Green Chem. 2011;13(10):2638.
11. Singh P, Kim Y-J, Zhang D, Yang D-C. Biological Synthesis

of Nanoparticles from Plants and Microorganisms. Trends Biotechnol. 2016;34(7):588-599.
12. Ahmed S, Ahmad M, Swami BL, Ikram S. A review on plants extract mediated synthesis of silver nanoparticles for antimicrobial applications: A green expertise. Journal of Advanced Research. 2016;7(1):17-28.
13. Thakkar KN, Mhatre SS, Parikh RY. Biological synthesis of metallic nanoparticles. Nanomed Nanotechnol Biol Med. 2010;6(2):257-262.
14. Mohammadinejad R, Karimi S, Iravani S, Varma RS. Plant-derived nanostructures: types and applications. Green Chem. 2016;18(1):20-52.
15. Suárez-Jacobo Á, Rüfer CE, Gervilla R, Guamis B, Roig-Sagués AX, Saldo J. Influence of ultra-high pressure homogenisation on antioxidant capacity, polyphenol and vitamin content of clear apple juice. Food Chem. 2011;127(2):447-454.
16. Venir E. Flavors of Dried Apples. Handbook of Fruit and Vegetable Flavors: Wiley; 2010. p. 515-529.
17. Vanaja M, Annadurai G. Coleus aromaticus leaf extract mediated synthesis of silver nanoparticles and its bactericidal activity. Applied Nanoscience. 2012;3(3):217-223.
18. Mittal AK, Chisti Y, Banerjee UC. Synthesis of metallic nanoparticles using plant extracts. Biotechnol Adv. 2013;31(2):346-356.
19. Goutam SP, Saxena G, Singh V, Yadav AK, Bharagava RN, Thapa KB. Green synthesis of TiO_2 nanoparticles using leaf extract of Jatropha curcas L. for photocatalytic degradation of tannery wastewater. Chem Eng J. 2018;336:386-396.
20. Wang J. Electrochemical Glucose Biosensors. Chem Rev. 2007;108(2):814-825.
21. Tian K, Prestgard M, Tiwari A. A review of recent advances in nonenzymatic glucose sensors. Materials Science and Engineering: C. 2014;41:100-118.
22. Kim K, Lim H, Park YM, Bae Y-S, Kim H-J. Highly Sensitive Non-Enzymatic Glucose Sensor Based on Metal-Organic Framework. ECS Meeting Abstracts. 2018;MA2018-02(56):2016-2016.
23. Liu S, Tian J, Wang L, Luo Y, Zhai J, Sun X. Preparation of photoluminescent carbon nitride dots from CCl4 and 1,2-ethylenediamine: a heat-treatment-based strategy. J Mater Chem. 2011;21(32):11726.
24. JCPDS — International Centre for Diffraction Data Task Group on Cell Parameter Refinement. Powder Diffr. 1986;1(1):66-76.
25. Linsebigler AL, Lu G, Yates JT. Photocatalysis on TiO_2 Surfaces: Principles, Mechanisms, and Selected Results. Chem Rev. 1995;95(3):735-758.
26. Rajakumar G, Rahuman AA, Roopan SM, Khanna VG, Elango G, Kamaraj C, et al. Fungus-mediated biosynthesis and characterization of TiO_2 nanoparticles and their activity against pathogenic bacteria. Spectrochimica Acta Part A: Molecular and Biomolecular Spectroscopy. 2012;91:23-29.
27. Roopan SM, Bharathi A, Prabhakarn A, Abdul Rahuman A, Velayutham K, Rajakumar G, et al. Efficient phyto-synthesis and structural characterization of rutile TiO_2 nanoparticles using Annona squamosa peel extract. Spectrochimica Acta Part A: Molecular and Biomolecular Spectroscopy. 2012;98:86-90.
28. Velayutham K, Rahuman AA, Rajakumar G, Roopan SM, Elango G, Kamaraj C, et al. Larvicidal activity of green synthesized silver nanoparticles using bark aqueous extract of Ficus racemosa against Culex quinquefasciatus and Culex gelidus. Asian Pac J Trop Med. 2013;6(2):95-101.
29. Wang Q, Chen Y, Zhu R, Luo M, Zou Z, Yu H, et al. One-step synthesis of Co(OH)F nanoflower based on micro-plasma: As an effective non-enzymatic glucose sensor. Sensors Actuators B: Chem. 2020;304:127282.
30. Yadav SK, Chandra P, Goyal RN, Shim Y-B. A review on determination of steroids in biological samples exploiting nanobio-electroanalytical methods. Anal Chim Acta. 2013;762:14-24.
31. Kang X, Mai Z, Zou X, Cai P, Mo J. A sensitive nonenzymatic glucose sensor in alkaline media with a copper nanocluster/multiwall carbon nanotube-modified glassy carbon electrode. Anal Biochem. 2007;363(1):143-150.
32. Zhang Y, Xu F, Sun Y, Shi Y, Wen Z, Li Z. Assembly of $Ni(OH)_2$ nanoplates on reduced graphene oxide: a two dimensional nanocomposite for enzyme-free glucose sensing. J Mater Chem. 2011;21(42):16949.
33. Si P, Huang Y, Wang T, Ma J. Nanomaterials for electrochemical non-enzymatic glucose biosensors. RSC Advances. 2013;3(11):3487.
34. Zhu X, Jiao Q, Zhang C, Zuo X, Xiao X, Liang Y, et al. Amperometric nonenzymatic determination of glucose based on a glassy carbon electrode modified with nickel(II) oxides and graphene. Microchimica Acta. 2013;180(5-6):477-483.